Available online at www.sciencedirect.com

SCIENCE DIRECT®

Global and Planetary Change 45 (2005) 35–49

GLOBAL AND PLANETARY CHANGE

www.elsevier.com/locate/gloplacha

Cenozoic landscape evolution of the Lambert basin, East Antarctica: the relative role of rivers and ice sheets

S.S.R. Jamieson[a,*], N.R.J. Hulton[a], D.E. Sugden[a], A.J. Payne[b,1], J. Taylor[b,1]

[a]Institute of Geography, School of GeoSciences, University of Edinburgh, Drummond St., Edinburgh, EH8 9XP, UK
[b]Bristol Glaciology Centre, School of Geographical Sciences, University Road, Bristol, BS8 1SS, UK

Received 1 September 2003; accepted 28 September 2004

Abstract

The inception of the Antarctic Ice Sheet at around 34 Ma followed a period of globally warm climatic conditions. The efficacy of glacial erosion since this time is modelled using BEDMAP Antarctic digital elevation data and seismically estimated offshore sediment volumes to derive a DEM of the preglacial topography. Using a GIS, sediment is 'virtually backstacked' on to the present-day topography under dynamic ice sheet conditions to produce a model of the preglacial landscape of the Lambert basin area in East Antarctica. Survival of a preglacial river valley system under the ice suggests that glacial modification of the Lambert region has been modest. The Lambert Graben has focussed erosion for the last 118 million years. Morphometric analysis of the modelled preglacial and present-day subglacial topographies shows parallels with present-day drainage systems in Africa and Australia. We calculate that average rates of glacial and fluvial erosion for the last 118 million years have been similar and are ca. 1–2 m Myr^{-1} and ca. 0.89–1.79 m Myr^{-1} respectively.

Keywords: Antarctic; Erosion; Evolution; Ice sheet; Landscape; Model

1. Aim

We aim to understand what has controlled the evolution of the East Antarctic bedrock landscape since the breakup of Gondwana at 118 Ma. We investigate the influences initially of fluvial processes and subsequently of glacial erosion processes by backstacking the latter products onshore. The rock volumes involved are estimated from sedimentary strata known from seismic surveys and drilling offshore.

Our investigation focuses on the Lambert region (Fig. 1) due to its well-defined topographic basin and because its erosion history is well constrained by studies of offshore sediment cores from continental shelf and fan environments in Prydz Bay. The importance of studying long-term landscape change

* Corresponding author. Tel.: +44 131 650 2565; fax: +44 131 650 2524.
E-mail address: S.Jamieson@ed.ac.uk (S.S.R. Jamieson).
[1] Fax: +44 117 928 7878.

0921-8181/$ - see front matter © 2004 Elsevier B.V. All rights reserved.
doi:10.1016/j.gloplacha.2004.09.015

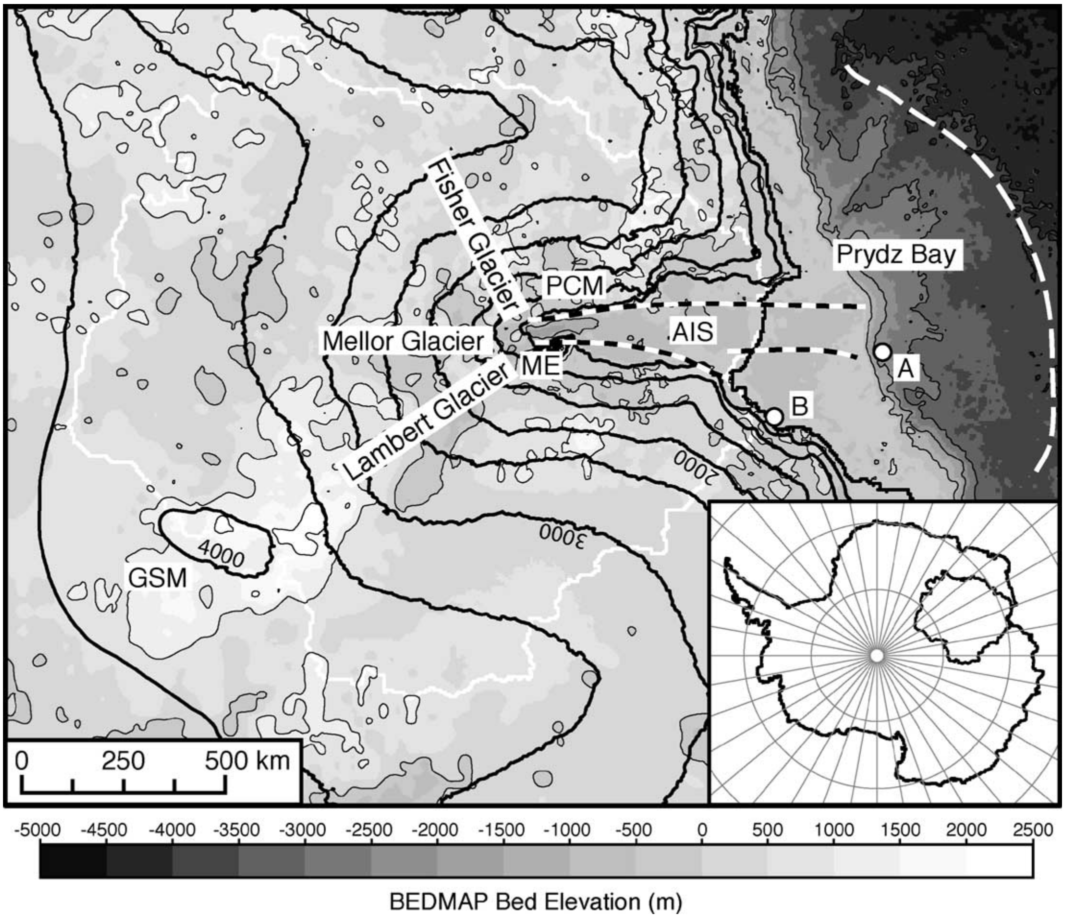

Fig. 1. The Lambert basin. Grey scale shading—BEDMAP bed data. AIS—Amery Ice Shelf, GSM—Gamburtsev Subglacial Mountains, ME—Mawson Escarpment, PCM—Prince Charles Mountains. White boundary—modern subglacial Lambert drainage divide. Bold contours—ice surface elevation (500 m intervals). Thin contours—bed elevation (1000 m intervals). Dashed lines—Lambert Graben. Long dashed white line—Prydz Channel Fan. Points (A) and (B)—profile position for Fig. 3. Inset—Antarctica and the Lambert basin, 10° grid spacing.

in this area is threefold. (1) It gives an insight into the topographic characteristics of the Lambert basin at the inception of the East Antarctic Ice Sheet (EAIS). This helps in understanding the influence of geomorphology on the origin of the EAIS and the subsequent efficacy of ice sheet modification of the Antarctic landscape. (2) It is possible to assess the processes of landscape evolution over geologic time scales by comparing average rates of glacial erosion with those of fluvial erosion. (3) Our focus on subglacial landscape evolution complements those studies that extrapolate long-term rates of change from study of glacier behaviour on short time scales.

2. Geographic and geologic setting

The Lambert ice basin comprises the largest outlet ice stream system in Antarctica (Stagg, 1985). Extending over an area of ca. 1.6 million km^2, the Lambert basin supports approximately 3.65 million km^3 of ice at the present day (ca. 10% of the total ice contained within the EAIS). Most ice flows through the tributary Fisher, Mellor and Lambert Glaciers into the Lambert Graben, the largest tectonic feature in East Antarctica (Fig. 1). Here, the ice flows north for ca. 500 km as the Lambert Glacier before terminating in the Amery Ice Shelf inland of the continental shelf in Prydz Bay (Ravich and Fedorov, 1982). Laterally constraining the Amery Ice Shelf to the East is the Mawson Escarpment, which rises steeply from the Lambert Graben and marks the edge of Princess Elizabeth Land. Along the entire length of the western margin of the graben, the Prince Charles Mountains constrain the floating ice, and inland of the graben peaks protrude above the main glaciers. The Lambert ice basin currently extends as far south as the Gamburtsev subglacial mountains, where Antarctic ice thicknesses are at their greatest (2500–3000 m).

The Lambert Graben represents a topographic low where bedrock elevations are more than 1000 m below present-day sea level. This contrasts with the 1500–2000 m mean altitude of the peaks in the adjacent Prince Charles Mountains (Mishra et al., 1999). The majority of the area is covered by the ice sheet, but many of the nunataks that protrude above the ice surface bear signs of glacial activity. Particularly well known in the Prince Charles Mountains is the glacially deposited Pagodroma Group well-consolidated successions of tillite comprising steep boulder slopes (Hambrey and McKelvey, 2000a,b).

It is important to consider the structural history of the study area—especially when the tectonic origin of the graben, its subsequent role as a sediment pathway, and its potential influence on the evolution of the EAIS is considered. Antarctica became a continent in its own right after the break-up of the Gondwana supercontinent. Bounding Antarctica in Gondwana were the present-day Australia, India, Africa, and South America, with the rifts between Antarctica, India, and Australia eventually leading to the formation of the current coastline around East Antarctica. The initial break-up of Gondwana along the East Antarctic coast has been constrained to between 127 and 118 Ma, as defined by magnetic anomaly M5-M0 time (Lawver et al., 1991). Australia was the final continent to separate from the East Antarctic coast at around 55 Ma, creating the Tasmanian Passage. Around 32.5 Ma, the Drake passage began to open between South America and Antarctica (Lawver and Gahagan, 1998). Based on these reconstructions, we assume that prior to ice sheet glaciation, the Lambert basin was subject to fluvial erosion since 118 Ma. The graben structure underneath the present-day Amery Ice Shelf was most likely to have formed during the Permian (Mishra et al., 1999) and may have extended into India (Fedorov et al., 1982). Within the Lambert basin area, the nature and rates of uplift since rifting have not been precisely determined, but it is known that the 20 million year old Mount Johnston Formation—part of the Pagodroma glaciomarine sequence—now rests at 1483 m above sea level (Hambrey and McKelvey, 2000a). The Pagodroma Group records the long-term uplift of at least the south wall of the Lambert Graben, with older glaciomarine sediments found at progressively higher levels (McKelvey et al., 2001). Therefore, over the past 20 million years uplift has been significant and may have been the result of either (or both of) tectonism related to faulting of the west shoulder of the graben or isostatic effects after removal of ice and/or bedrock load.

2.1. Climate history

The present-day climate of Antarctica is characterised by a cold polar environment. However, in early Oligocene Antarctica, evidence from the CIROS-1 core drilled offshore of the Transantarctic Mountains suggests that the climate was sufficiently warm to support a beech forest (Mildenhall, 1989). Indeed, at this time, planetary temperatures were 3–4 °C warmer than at present (Crowley and Kim, 1995). Decreasing temperatures into the Miocene meant that vegetation survived only in favoured locations as sparse tundra scrub (Raine and Askin, 2001). This cooling trend coincides with changes in the clay mineralogy of sediment extracted from both the Cape Roberts and CIROS-1 cores. Smectites associated with forest soils give way to chlorite and illite, indicating the transition to a polar environment (Ehrmann, 2001). Evidence in the Victoria Land sector of the Transantarctic Mountains has been used to indicate that hyperarid polar conditions have prevailed for at least the last 13.6 million years since the mid-Miocene ice sheet maximum (Denton et al., 1993; Sugden et al., 1995; Marchant et al., 1996).

It has been argued that climatic conditions suitable for ice growth across Antarctica were introduced with the opening of the Drake Passage at ca. 32.5 Ma, allowing increased circumpolar oceanic and atmospheric circulation to cool the continent (Kennett, 1977; Lawver and Gahagan, 1998). Recent research, however, suggests that the effects of the opening of

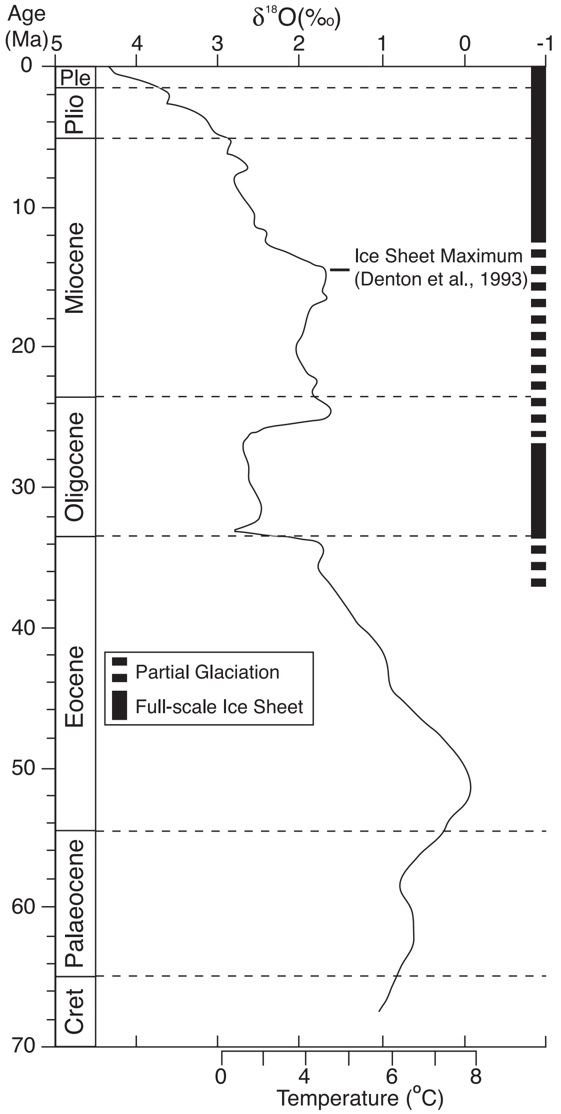

Fig. 2. Global deep-sea oxygen isotope curve (after Zachos et al., 2001). This curve is a 5-point running mean and is curve fitted with a locally weighted mean.

these southern ocean seaways may not have been felt climatically until after the inception of the ice sheet, with declining atmospheric CO_2 concentrations perhaps being the cause of ice sheet initiation (DeConto and Pollard, 2003). The Lambert Graben is thought to be one of the first sites to discharge ice, and by ca. 34 Ma, it is generally agreed that a full ice sheet existed (Barrett, 1996). Supporting this, Zachos et al. (1992, 2001) indicate on the basis of oxygen isotope records that a sharp step in cooling occurred at 34 Ma, and that it was likely to be accompanied by significant ice growth at that time (Fig. 2). According to Zachos et al. (2001), there may have been a period of warming in the late Oligocene and early Miocene, but the amplitude and even existence of this are uncertain.

In Prydz Bay, the glacial and preglacial history of the Lambert basin is recorded through deposition of sediment on the continental shelf beginning in the Eocene to early Oligocene (Fig. 3; Cooper et al., 1991; Hambrey et al., 1991, 1992). The greatest accumulation of flat-lying sediment occurs nearer the shelf break, whereas the inshore area has been subjected to erosion during ice advances and displays less sediment accumulation. As a result, water depths range from over 800 m in the inner shelf to 400 m on the outer shelf (Hambrey et al., 1992). Investigation of sediment cores indicates that deposition is largely continental in the inner parts and terrestrial–marine glacigenic closer to the shelf edge (Hambrey, 1991). Within the cores, it is possible to identify the switch from preglacial fluvial and deltaic processes to deposition of water-lain tills when grounded ice reached the palaeo-shelf break (Hambrey et al., 1992).

During the late Miocene/Pliocene, a large fan—the Prydz Channel Fan—developed. Extending over the continental shelf edge, the fan is associated with the Prydz Channel formation (O'Brien et al., 2001) and

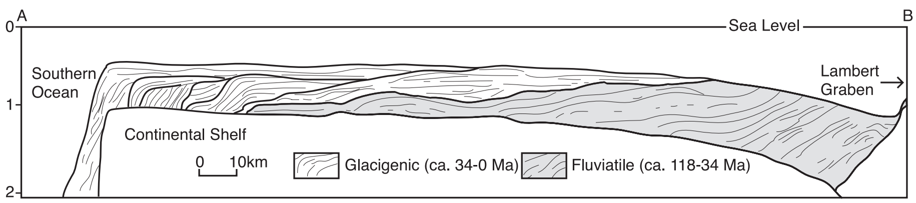

Fig. 3. Seismic profile of sediments in Prydz Bay (after Cooper et al., 1991), depth is two-way travel time. Sediment volumes were estimated from glacial/fluvial facies boundaries located in ocean cores from ODP legs 119 and 188 (Stagg, 1985; Cooper et al., 1991, 2001; O'Brien et al., 2001). For profile position, see Fig. 1.

the development of the Lambert Glacier as a fast-moving ice stream at the western margin of Prydz Bay. The fan grew largely through the input of basal debris, partly made up of Pagodroma Group sediments at times when the grounding line was at the shelf edge, with gravity processes redistributing the material over time (Hambrey and McKelvey, 2000b; O'Brien et al., 2001).

3. Approach and methods

Our approach is to identify where erosion has occurred under the EAIS and to reconstruct the landscape at the ca. 34 Ma glacial transition. We use 5-km resolution data of present-day bed topography, ice thickness, and ice surface from the BEDMAP project to represent the existing subglacial topography and ice conditions (BEDMAP Consortium, 2002). We also employ seismically estimated offshore sediment volumes as a guide for backstacking, and using a geographical information system (GIS), we produce modelled subglacial topographies for various time steps extending back to the inception of the full ice sheet. The resulting topographies, in the form of digital elevation models (DEMs), are analysed morphometrically using GIS and the results used to test the degree of landscape change as a result of ice sheet glaciation.

3.1. Model specification

Backstacking is defined as the allocation of a quantity of previously eroded sediment to the positions from which it originated (Fig. 4). The essential problem is to determine at progressive time steps in the past where sediment has been removed by glacial erosion. To achieve this, we make simplifying assumptions about rates of glacial erosion based on the form of the glacier and its bed temperatures. We use an existing 3D model of the ice sheet to derive the basal temperature regime under present glacial conditions (Siegert et al., 2005). The erosion rate (and hence, the proportion of backstacked material) is set to zero where the bed is frozen because abrasion is negligible in this situation (Boulton, 1972). Where the bed reaches pressure melting point, erosion rate varies as a linear function of basal shear stress. Basal shear stress is expressed using conventional glaciological theory as a nonlinear function of ice thickness and surface gradient (Paterson, 2001). In practice, for each time step, we integrate total erosion rates across the basin and then normalise erosion rates at individual locations. We thus produce a varying distribution of erosion rates whose integral is always one and multiply these by a fixed quantity of sediment for that time step. Therefore, we control the total amount of sediment incrementally backstacked but allow a spatially varying distribution based on glaciological principles. As the bed surface evolves, we recalculate ice thicknesses and shear stress assuming the ice surface profile remains static and reassign relative erosion rates on this basis. Nonflexural isostatic adjustment is calculated at the final time step to account for both ice thickness change and for modification of the bed elevation as sediment is backstacked. Ideally, we would permit the glacier form and basal thermal regime to evolve in response to the changing bed profile, but as a further simplification, we assume that the surface form and bed temperatures of the ice sheet remain static. In addition, we assume that the bedrock is equally erodible, that the Lambert basin is a closed system, and that the sediment presently accumulated in Prydz Bay was derived only from the Lambert basin.

To constrain the model temporally and to assign a total for backstacked sediment, offshore sedimentology is used to identify the boundary between fluvial and glacial sediments. Based upon seismic interpretations of offshore morphology and stratigraphy on the Prydz Bay shelf and upper slope (Stagg, 1985; Cooper et al., 1991, 2001; O'Brien et al., 2001), estimates for sediment output from the Lambert system were made from digitised isopach data and contour maps. Approximate calculations of glacially derived sediment volume suggest that ca. 54,000 km^3 has been deposited since the initiation of glacial conditions in East Antarctica. Prior to this, a further 98,000 km^3 of largely fluviatile sediment was deposited. These estimates are used to limit the amount of material backstacked during the model run. Although the individual time steps do not refer explicitly to geologic time, the end point of the model is assumed to be the start of ice sheet glaciation at ca. 34 Ma.

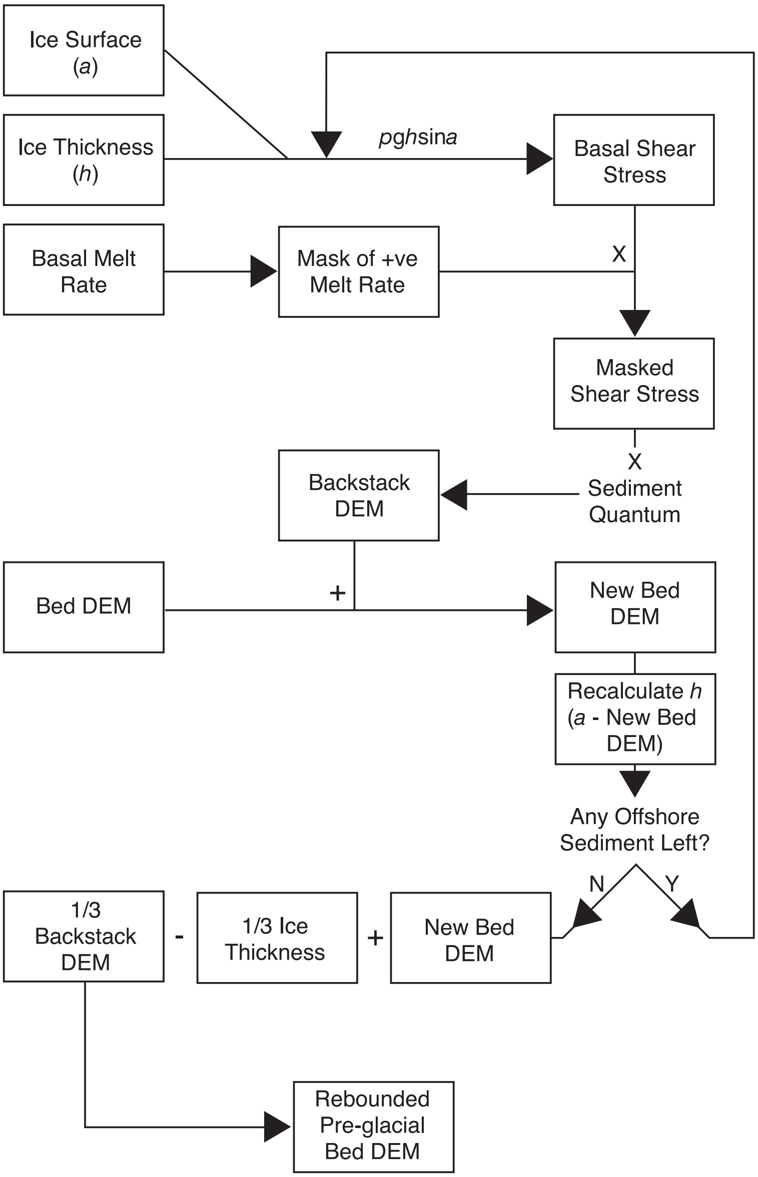

Fig. 4. Flow diagram of backstacking methodology.

3.2. GIS, hydrological, and morphometric analysis

Having created a 'preglacial' surface on the basis of backstacked sediment and isostatic readjustment, we evaluate whether this represents a viable fluvial system. We utilise hydrological modelling methods for cell-based DEMs as a means of establishing the pattern of any valley network. The idea is to consider whether some erosion scenarios imply a more coherent fluvial system than others. The morphometry of the preglacial system is also compared with other present-day fluvial catchments.

We employ ArcGIS (ESRI, 2002) which uses a local drain direction (ldd) method. This searches a window of three-by-three cells and assumes a river will flow towards the neighbouring cell with the lowest

Table 1
Derived morphometric parameters used for the subglacial Lambert basin

Parameter	Description
Basin	
Area	Area of the basin
Perimeter	Perimeter of the basin
Hypsometry	Curve expressing proportion of total basin area to total basin elevation
Hypsometric integral	Percentage area under the hypsometric curve
Circularity	Basin area/the area of a circle with the same perimeter as the basin
Basin length	Maximum basin length measured from the mouth
Elongation ratio	Diameter of a circle with the same area as the basin/basin length
Elevation mean	Mean elevation across the basin
Relief	$\mathrm{Elevation}_{max} - \mathrm{elevation}_{min}$
Network	
Drainage density	Mean length of stream channels/basin area
Bifurcation ratios	No. of streams of order_0/No. of streams of order_{+1}
Mean bifurcation	Mean of all bifurcation ratios

absolute elevation (Fairfield and Leymarie, 1991; Burrough and McDonnell, 1998). This is applied to all cells over a hydrologically continuous DEM. Often, there may be no neighbouring cell with a lower elevation, and in this case, the central cell is 'filled' until it is the same elevation as the lowest adjacent cell. This pit filling technique introduces implied lakes into the drainage system and ensures that the DEM is hydrologically sound. On a large scale, these lakes are likely to represent real world features, although on a smaller scale (ca. single cell lakes), these features may be artifacts of the DEM (Tribe, 1992; Martz and Garbrecht, 1998). The ldd method is simple, reproducible, and requires only a threshold for inferred flow to be entered as a parameter. In the case of the Lambert basin, the valley networks were derived using an upstream area equivalent to 2500 km^2 (100 cells) to maintain intercomparability between modelled time steps. Defining a threshold is necessary because it allows the presence of a river at a certain scale to be inferred. Too small a threshold and the network will become increasingly complex, too large and only the biggest valleys will be identified. Using the drainage basin as an easily definable unit of the landscape, various morphometric parameters were extracted (Table 1). It should be noted that drainage density is used here as a comparative measure between DEMs rather than a method of comparison with previously studied landscapes because it is not scale-independent and so cannot be compared directly to densities found in the literature which are derived using differing thresholds. Mean bifurcation ratios avoid scaling factors associated with drainage extraction and, hence, can be used for comparison.

3.3. Data

Most of the data are drawn from the BEDMAP Antarctic Database of 5-km resolution DEMs (BEDMAP Consortium, 2002), and this is supplemented by a grid of present-day modelled basal melt-rate data. Three different BEDMAP data sets are employed—bed elevation, ice surface, and ice thickness. These data are a collation of over 50 years of surveying in

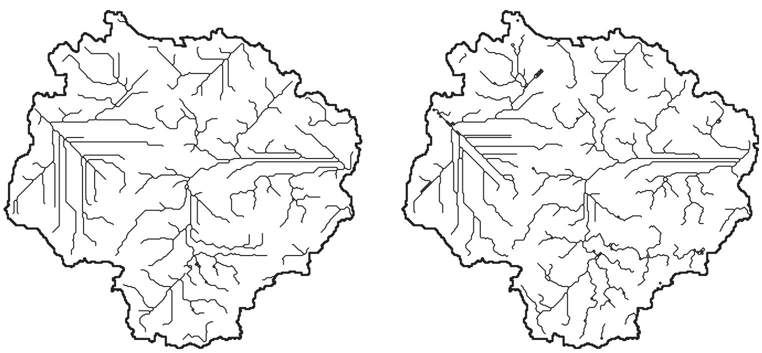

Fig. 5. The similarity of the original BEDMAP drainage structure (left) to drainage extracted from data with added random error (right). This points to the robustness of the BEDMAP bed elevation data to local error.

and around Antarctica brought together in a suite of integrated topographical models aimed specifically at providing a basis for time-dependent ice sheet modelling (Lythe et al., 2001). The basal melt-rate for the present day was modelled on a 20-km grid scale using a 3D ice sheet model (Siegert et al., 2005) and subsequently interpolated onto a 5-km grid to maintain consistency with the BEDMAP data.

Although the nominal resolution of the BEDMAP data is 5 km, only in very few parts of the continent are the original data dense enough to justify this level of detail within the bed elevation data set. Large gaps (sometimes greater than 100 km) in the data are filled using inverse distance weighted interpolation (Lythe et al., 2001), with the result that a visible reduction in data quality is apparent in these areas as hummocky topography. Despite this, the data set is more reliable than earlier maps (e.g., see Drewry, 1983). The absolute positional horizontal accuracy of the BEDMAP grounded bed DEM generally varies between 100 and 300 m although it can be as high as 10 km in some inland areas. The absolute vertical accuracy of

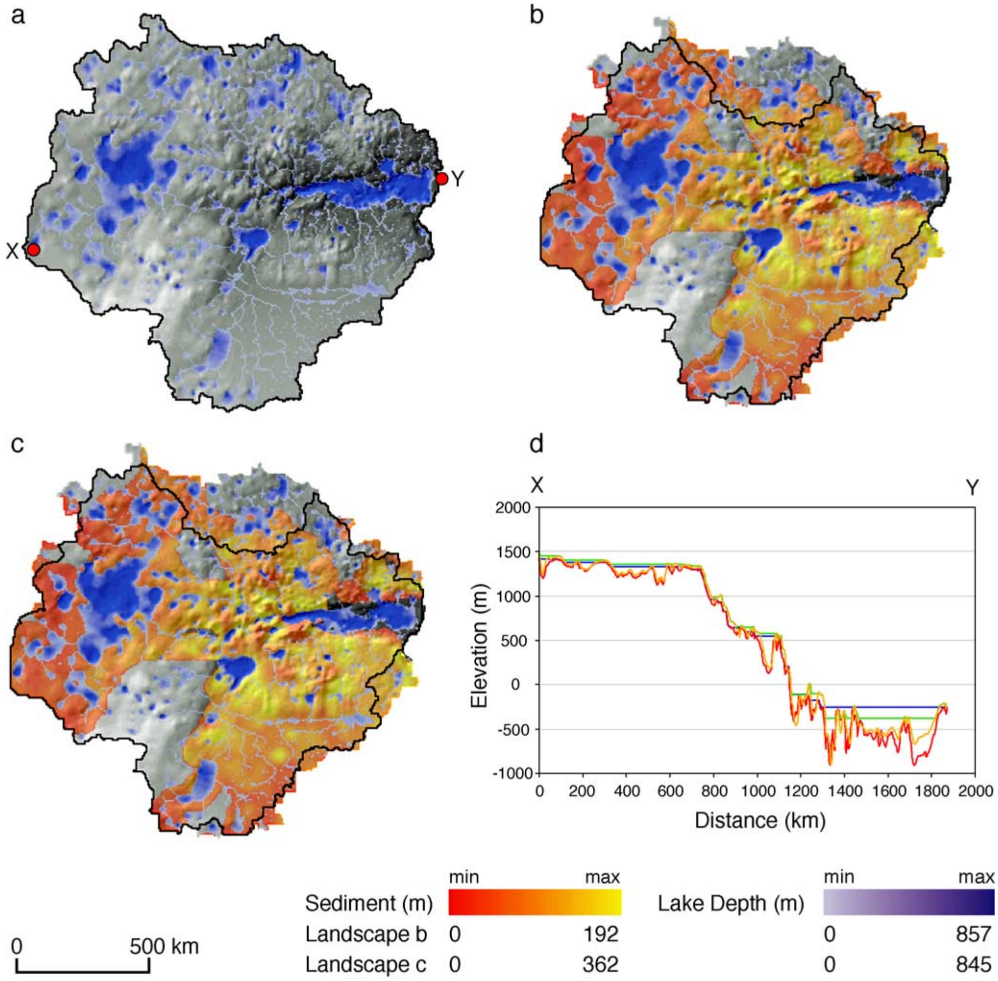

Fig. 6. Topographies and stream profiles in the Lambert basin. Grey scale data—shaded relief, red to yellow—backstacked sediment thickness, blue areas and lines—lake depth and river network, black line—outline of Lambert basin. (a) Present-day topography and drainage assuming no ice sheet and complete isostatic recovery. (b) The preglacial Lambert basin with backstacked sediment in place. (c) The preglacial Lambert system with doubled sediment in place. (d) Stream profiles (*X*–*Y*)—red and blue lines profile through topography (a), orange and green lines profile through topography (c)—flat lines show implied lake surfaces, jagged lines show absolute bedrock elevation.

the grounded ice sheet model is between 150 and 300 m in most areas (Lythe et al., 2001).

To test the effect of this vertical error, a flow direction network was derived for the original BEDMAP data. Random error within the specified accuracy limits was then added to the bed DEM, and direction of flow was again modelled. This was done 10 times, and the resultant flow direction grids were then compared numerically to identify the number of cells in which flow had changed direction due to the addition of random error. Even when local flow direction changed in almost 55% of the cells, the derived river networks were remarkably similar (Fig. 5). This occurs because the scale of network derivation is larger than the single cell with 100 cells being used to define a river. Hence, we assume the BEDMAP data are adequate as the basis for deriving the overall valley networks because the hydrological model is robust to localised errors.

4. Present-day topography assuming no ice sheet

As an initial step prior to backstacking, the present-day ice load was removed, and the BEDMAP data allowed to rebound isostatically using a nonflexural adjustment, the intention being that this data set would be used as a comparison to backstacked topographies at a later stage. Fig. 6a shows the resultant topography and associated drainage network for the present day after complete removal of the EAIS. It reveals a single fluvial drainage basin with an area of almost 1.6 million km^2 flowing into Prydz Bay through the Lambert Graben. This system is characterised by over 4000 m of relief and a mean bifurcation ratio of 3.7 (Table 2). The latter ratio is typical of a dendritic pattern and indicates that the basin is not over-elongated, and that it is relatively unaffected by gross geological structure. In addition, it appears that a major lake exists in the far south of the Lambert system covering an area of ca. 4.2×10^4 km^2.

The shape measurements of circularity and elongation (0.28 and 1.65, respectively) indicate that the Lambert basin is close to being circular. The hypsometric curve (Fig. 7) shows that a relatively large proportion of the basin area lies at intermediate altitudes. Supporting this, the hypsometric integral (percent area under the hypsometric curve) is 59.8%, although this figure is skewed by the inclusion of the submarine graben in the measurements. With the exclusion of the submerged graben from the calculations, the hypsometric integral becomes 45.3%, indicating more land closer to sea level. The hypsometric curve for the present day with the graben removed confirms this lower area elevation distribution (Fig. 7). The lack of sharp changes in the hypsometric curve indicates that, if base-level change has occurred in the past, it has been gradual with erosion keeping pace with the uplift.

5. Preglacial topography

Using the offshore sediment volume estimates as the limiting factor (Fig. 3), the backstacking model (Fig. 4) was run to determine the 34-Ma preglacial

Table 2
Morphometric data from the Lambert, Orange, and Murray basins[a]

Measurement	Present	Preglacial	Preglacial (2×)	Preglacial (10×)	Orange	Murray
Basin area (million km^2)	1.58	1.31	1.30	1.19	1.02	1.22
Basin perimeter (km)	8400	7850	7880	7550	6186	6945
Basin length (km)	1622	1551	1551	1533	1536	1657
Hypsometric integral (%)	59.8 (45.3)	59.7 (45.7)	59.8 (46.1)	60.9 (49.6)	37.8	14.2
Circularity ratio	0.28	0.27	0.26	0.26	0.34	0.32
Elongation ratio	1.65	1.61	1.62	1.57	1.28	1.33
Mean bifurcation	3.7	3.4	3.5	3.4	3.5	2.9
Mean elevation (m)	1226	1221	1233	1317	1209	250
Relief (m)	4173	4120	4108	4010	2957	1756
Drainage density (km km^{-2})	0.0153	0.0152	0.0150	0.0153	0.0152	0.0172

[a] Bracketed values indicate hypsometric integral after removal of the graben below sea level.

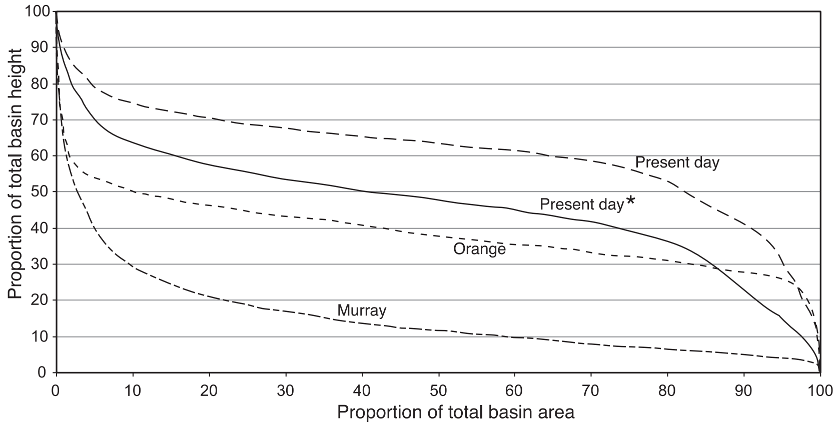

Fig. 7. Comparative hypsometric curves. The present-day* and Orange curves show similar gradients above ca. 35% of the basin elevation. This indicates comparable area elevation distributions across ca. 80% of both the landscapes areas. *Hypsometry measured above sea level only.

topography for the Lambert basin. The isostatically rebounded topography for the final time step was morphometrically compared to the present rebounded BEDMAP bed DEM.

Fig. 6b identifies the distribution of backstacked sediment in the Lambert basin and the valley network associated with the modelled preglacial surface. Much of the sediment has been distributed in a wide arc around the head of the graben, with added sediment volume tailing off towards the fringes of the basin in all directions. Most sediment backstacking and, hence, past erosion occurs in the subglacial valleys converging on the head of the graben where the Fisher, Mellor, and Lambert Glaciers currently flow, and a large amount of sediment is assigned to the area inland of the Mawson Escarpment. The main graben does not receive any sediment because the ice remains afloat in the model, and hence, shear stress (backstacking) remains at zero throughout the time steps. The other areas which show no change are those that are never above pressure melting point according to our model.

The valley network shows a remarkable similarity to that of the present-day rebounded drainage (Fig. 6a). There is one major dendritic basin with a number of small catchments on the periphery of the Lambert, and in common to the present-day topography, a large lake is present to the south. The implication is that the present Mellor and Lambert Glaciers were significant topographic features 34 million years ago and channelled the system into the Lambert Graben. The headwaters of the smaller basins along the western and northern margins of the study area correspond to small areas of increased elevation through backstacked sediment positioning.

Morphometric analysis of the preglacial surface and valley network suggests that the landscape has not undergone significant change since the early Oligocene. The largest change is in the configuration of the largest basin within the Lambert system, which shows an increase over time from 1.31 to 1.58 million km^2 in area (Table 2). Accordingly, the perimeter and length of the basin also adjusts, but the circularity and elongation ratios, which describe basin shape, show barely any change. The hypsometric integral too adjusts only slightly, thus indicating that the distribution of area to elevation has not altered over time despite the drainage capture that is suggested by the increase in basin area. Hypsometric curves display very little change, maintaining a similar altitudinal distribution before and after glaciation. Total relief has increased during glaciation but only marginally by ca. 53 m to 4173 m as a result of isostatic adjustment after removal of material, and the mean elevation has increased marginally. Bifurcation ratio data indicate that slight reorganisation of drainage has occurred in the larger rivers, most of which are located within the band adjacent to the graben headwall. Overall, however, mean bifurcation ratios remain within the range expected for a dendritic river system, and drainage densities are unchanging in our experiments. The lack of significant difference in the majority of parameters over time suggests that most reorganisation of the drainage system is confined to change on a scale smaller than 100 km^2.

6. Sensitivity

It is important to note that, although a division between the fluvially and glacially derived sediment is discernible in the offshore records from ODP legs 119 (Hambrey, 1991) and 188 (O'Brien et al., 2001), it is unclear how much fluvially derived sediment was deposited onshore and then removed by the ice sheet. This introduces uncertainty into the sediment record used here to define end member topographic states and, hence, an element of error into the model output for the preglacial land surface. Furthermore, it is clear that the Lambert system was not a closed system over the past 34 million years. Antarctic sediment is found far beyond continental slope in the form of ice rafted debris (Kennett and Brunner, 1973) and as clay mineral assemblages (Robert and Kennett, 1992) so that any estimate of actual sediment volumes removed from Antarctica will inevitably be a minimum. To test the sensitivity of our model, we carried out two further backstacking experiments—firstly, doubling the volume used to constrain the backstacking and, secondly, multiplying the volume by a factor of 10.

As can be seen in Fig. 6c, the doubled sediment is effectively backstacked in the same pattern as that of the previous experiment, with sediment depths being higher over a greater distance from the graben. The valley network too is very close in form to that of the initial preglacial experiment (Table 2) and includes the prominent southern lake feature. The network morphometry parameters (such as bifurcation ratios and stream frequency) differ very little from the initial backstack run. Other morphometric measures are also similar. For instance, the hypsometric integral increases only slightly in the doubled sediment run. Backstacking 10 times the volume of sediment causes an increased mean elevation and a decrease in relief, within a slightly smaller Lambert basin. The valley network, however, displays similar drainage density and bifurcation ratio characteristics to the previous experiments (Table 2).

7. Discussion

7.1. The preglacial Lambert topographies

The model reveals a coherent drainage system under the present-day East Antarctic Ice Sheet. Furthermore, we note that this system has not changed significantly in form since Oligocene times and would change little even if we test our model assuming 90% of the sediment originating from the Lambert has been lost. The broad pattern of erosion is consistent with what might be expected under ice sheet conditions with the sediment being placed in areas of overdeepening and particularly in the present-day Lambert, Mellor, and Fisher Valleys. Fig. 6d shows a stream profile through the present-day and the double backstacked topographies and supports our findings that sediment is placed in areas where preexisting topographic hollows are located. The reason for this is that the ice surface is at its steepest and thickest in these areas allowing high basal shear stresses to develop. It is not surprising, therefore, that the macroscale drainage pattern has survived even under prolonged glacial conditions.

The bedrock drainage pattern in this part of East Antarctica is similar to that of a number of large drainage systems found in the world today—in particular, the Murray basin of Australia and the South African Orange river. Both of these rivers are on rifted margins of Gondwana, are over 1500 km in length, and are dendritic at this scale. Morphometric measurements taken from ca.10-km resolution DEMs (NOAA, 1998) of these catchments are presented in Table 2 and agree with previous morphometric analysis of these drainage systems (Summerfield and Hulton, 1994). Both of these basins have lower relief than the Lambert but share similar network measurements despite their vastly different environmental histories over the past 34 million years. The hypsometric curves suggest a lower area altitude distribution in the Orange and Murray basins when compared to that of the Lambert basin (Fig. 7), but their shapes are very similar, particularly in their upper elevation portions. This suggests that the impact of glacial conditions upon East Antarctica has been focussed to the valley scale, and that plateau areas in the Lambert area have remained relatively unmodified by glacial activity.

We consistently identify a large lake in the southern portion of the basin. This lake is such a size (ca. 4.2×10^4 km^2) that it would be the sixth largest freshwater body in the world today between Lake Michigan, USA, and Lake Tanganyika, Tanzania. The effect of this lake on the long-term evolution of the Lambert basin is unclear although sediment input (and hence erosion) to the system downstream of the lake will have been significantly reduced after lacustrine deposition. This is particularly true because the lake has only one outflow point and hence would require to be full to allow any input to the lower portions of the Lambert drainage system.

7.2. Glacial vs. fluvial

Calculations of offshore sediment volume from the Prydz Bay shelf and the Prydz Channel Fan indicate that up to 9.8×10^4 km^3 of preglacial and 5.4×10^4 km^3 of glacigenic material have been excavated from the Lambert basin assuming a closed system (after Stagg, 1985; Cooper et al., 1991, 2001; O'Brien et al., 2001). Allowing for loss of sediment from the shelf and fan, we assume that up to double this amount of sediment may have originated in the Lambert basin. The glacigenic material has been deposited over the past 34 million years and the fluvial sediment over the previous 84 million years between the break-up of Gondwana and the initiation of the EAIS. Using the volume of the Prydz Bay shelf and Prydz Channel Fan at one extreme and its doubling at the other, we calculate a range of average erosion rates for the present-day and preglacial Lambert basins. We estimate that average fluvial erosion rates range between 0.89 and 1.79 m Myr^{-1} and average glacial rates between 1 and 2 m Myr^{-1}. These rates are significantly lower than those previously calculated for the Orange river by Rust and Summerfield (1990) although their averaged rate of ca. 12 m Myr^{-1} hides the fact that rates may have been as low as 7–9 m Myr^{-1} during later stages. The implication is that rates of erosion in the Lambert basin have been extremely low. Furthermore, rates of fluvial vs. glacial erosion in this region are roughly comparable. This latter finding is supported by other data for denudation rates under glacial and fluvial conditions (Summerfield and Kirkbride, 1992).

7.3. Limitations

The results of our experiments suggest that the Lambert Graben has been the preeminent forcing factor behind the development of the preglacial valley systems and their later exploitation by the ice sheet. Our assumptions of static basal melt distribution and ice surface, however, mean that we have been unable to model the erosional evolution of the graben itself. Instead, our calculations of backstacking were based on the characteristics of the present EAIS. In reality, however, the early ice sheet filled the graben and extended to the outer shelf where it discharged ice and debris from a wide front. At some early stage, grounded ice would have been capable of eroding the graben floor. Furthermore, the evolution of melting at the base of the EAIS would have smoothed the sediment backstacked here because of local changes to topography resulting from erosion. The cause of increased mean elevation after glaciation in our model is an additional consequence of assuming a static ice sheet surface. This is largely a function of isostatic adjustment because the preglacial topography rebounds less than the present-day topography due to the thinner ice that remains after sediment backstacking. In addition, we assume that the modelled ice sheet is consistent with current temperatures and is thus not reacting to past changes in surface temperature. Hence, the conclusions of this paper are no more than a first step. We are presently addressing the second step of relating the backstacking to a dynamically evolving ice sheet model. However, with the exception of the submerged Lambert Graben itself, the introduction of a continuously adjusting basal melt distribution is not likely to have changed the modelled patterns of erosion significantly.

In the development of our model, we imposed a closed system of deposition in order that we could use offshore sediment volumes to constrain our backstacking. This assumption is reasonable because transport of glacial sediment beyond the Prydz Channel Fan as ice-rafted debris (IRD) and in solution is not likely to be significant. For example, Dowdeswell and Dowdeswell (1989) estimate sedimentation from icebergs in present-day Spitsbergen to be the equivalent to 1 mm a^{-1}. Icebergs can travel many hundreds of kilometres, but there is a strong decay relationship of IRD sedimentation with distance from the ice front (Ruddiman, 1977; Dowdeswell et al., 1995). Assuming that most sediment within icebergs is near their base and that this can melt out within a few days of calving (Dowdeswell and Dowdeswell, 1989), then the proportion of total sediment originating from the Lambert and travelling beyond the fan will be insignificant. Indeed, Drewry (1986) presents a hypothetical debris release scheme suggesting that the majority of sediment is dropped by an iceberg within 200 km of the ice margin, and that the iceberg is essentially clean at a distance of 400 km. Sediment transport in solution is difficult to account for although studies of the Murray and Orange systems indicate that chemical denudation under fluvial conditions accounts for 9.7–14.5% of total denudation, respectively (Summerfield and Hulton, 1994). Therefore, even if we assumed that all ice-rafted debris and sediment in solution was carried past the Prydz Channel fan, our approach of doubling sediment volumes will easily encompass any combined sediment deposited out with our study area through such modes of transport. Given this evidence, our conclusion that overall erosion rates have been extremely low appears robust.

8. Conclusions

(1) A preglacial fluvial landscape survives beneath the Lambert basin area of the East Antarctic Ice Sheet. Morphometry suggests that it is a large river basin similar to the present Orange River in South Africa.

(2) The East Antarctic Ice Sheet has eroded the preexisting landscape selectively. Significant modification is confined to the valleys converging on the head of the Lambert Graben and in the graben itself. The adjustment of the uplands and of areas further inland of the graben is minimal.

(3) Over 118 million years, the Lambert Graben has acted as the principal forcing factor upon erosional pathways in the region, firstly under fluvial conditions and subsequently under ice sheet conditions over the last 34 million years.

(4) Inferred minimum glacial and preglacial erosion rates are remarkably similar, ranging between ca. 1–2 and ca. 0.89–1.79 m Myr^{-1}. This supports arguments that it is the tectonic topography and relief that controls denudation rates over millions of years rather than a change from fluvial to glacial conditions.

Acknowledgements

Many thanks to Peter Barrett and an anonymous reviewer for their useful comments on this manuscript. This work was supported by the Natural Environmental Research Council, UK.

References

Barrett, P.J., 1996. Antarctic palaeoenvironment through Cenozoic times—a review. Terra Antarctica 3, 103–119.

BEDMAP Consortium, 2002. http://www.antarctica.ac.uk/aedc/bedmap/. BEDMAP home page—A new ice thickness and subglacial topographic model of the Antarctic. Last Accessed: 11th November 2003.

Boulton, G.S., 1972. The role of thermal regime in glacial sedimentation. In: Price, R.J., Sugden, D.E. (Eds.), Polar Geomorphology. Special Publication Institute of British Geographers, vol. 4, pp. 1–19.

Burrough, P.A., McDonnell, R.A., 1998. Principles of Geographical Information Systems: Spatial Information Systems and Geostatistics. Oxford University Press.

Cooper, A., Stagg, H., Geist, E., 1991. Seismic stratigraphy and structure of Prydz Bay, Antarctica: implications from ODP Leg 119 drilling. In: Barron, J.B., Larsen, B. (Eds.), Ocean Drilling Program Leg 119, Scientific results, College Station, Texas, pp. 5–25.

Cooper, A.K., O'Brien, P.E., ODP Leg 188 Shipboard Scientific Party, 2001. Early stages of East Antarctic glaciation—insights from drilling and seismic reflection data in the Prydz Bay region. In: Florindo, F., Cooper, A.K. (Eds.), The Geologic Record of the Antarctic Ice Sheet from Drilling, Coring and Seismic Studies, Extended abstracts. Quaderni di Geofisca, vol. 16, pp. 41–42.

Crowley, T.J., Kim, K.-Y., 1995. Comparison of long term greenhouse projections with the geologic record. Geophysical Research Letters 22 (8), 933–936.

DeConto, R.M., Pollard, D., 2003. Rapid Cenozoic glaciation of Antarctica induced by declining atmospheric CO_2. Nature 421, 245–249.

Denton, G.H., Sugden, D.E., Marchant, D.R., Hall, B.L., Wilch, T.I., 1993. East Antarctic ice sheet sensitivity to Pliocene climatic change from a dry valleys perspective. Geografiska Annaler 75A (4), 155–204.

Dowdeswell, J.A., Dowdeswell, E.K., 1989. Debris in icebergs and rates of glaci-marine sedimentation: observations from Spitsbergen and a simple model. Journal of Geology 97, 221–231.

Dowdeswell, J.A., Maslin, M.A., Andrews, J.T., McCave, I.N., 1995. Iceberg production, debris rafting, and the extent and thickness of Heinrich layers (H-1, H-2) in North Atlantic sediments. Geology 23, 301–304.

Drewry, D.J., 1983. Antarctica: Glaciological and Geophysical Folio. Scott Polar Research Institute, Cambridge, England.

Drewry, D.J., 1986. Glacial Geologic Processes. Edward Arnold, London.

Ehrmann, 2001. Variations in smectite content and crystallinity in sediments from CRP-3, Victoria Land Basin, Antarctica. Terra Antartica 8 (4), 533–542.

ESRI, 2002. ArcGIS 8.2. Environmental Systems Research Institute, Redlands, CA.

Fairfield, J., Leymarie, P., 1991. Drainage networks from grid digital elevation models. Water Resources Research 27 (5), 709–717.

Fedorov, L.V., Ravich, M.G., Hofmann, J., 1982. Geologic comparison of southeastern peninsular India and Sri Lanka with a part of East Antarctica (Enderby Land, MacRobertson Land and Princess Elizabeth Land). In: Craddock, C. (Ed.), Antarctic Geoscience. Symposium on Antarctic Geology and Geophysics. University of Wisconsin Press, Madison, WI, pp. 73–78.

Hambrey, M.J., 1991. Structure and dynamics of the Lambert Glacier–Amery Ice Shelf system: implications for the origin of Prydz Bay sediments. Proceedings of the Ocean Drilling Program. Scientific Results, vol. 119. Ocean Drilling Program, College Station, TX, pp. 61–75.

Hambrey, M.J., McKelvey, B., 2000a. Major Neogene fluctuations of the East Antarctic ice sheet: stratigraphic evidence from the Lambert Glacier region. Geology 28, 887–890.

Hambrey, M.J., McKelvey, B., 2000b. Neogene Fjordal sedimentation on the western margin of the Lambert Graben, East Antarctica. Sedimentology 47, 577–607.

Hambrey, M.J., Ehrmann, W.U., Larsen, B., 1991. Cenozoic glacial record of the Prydz Bay continental shelf, East Antarctica. Proceedings of the Ocean Drilling Program. Scientific Results, vol. 119. Ocean Drilling Program, College Station, TX, pp. 77–133.

Hambrey, M.J., Barrett, P.J., Ehrmann, W.U., Larsen, B., 1992. Cenozoic sedimentary processes on the Antarctic continental margin and the record from deep drilling. Zeitschrift fur Geomorphologie. Supplementband 86, 77–103.

Kennett, J.P., 1977. Cenozoic evolution of Antarctic glaciation, the circum-Antarctic Ocean and their impact on global palaeoceanography. Journal of Geophysical Research 82, 3843–3860.

Kennett, J.P., Brunner, C.A., 1973. Antarctic Late Cenozoic glaciation: evidence for initiation of ice rafting and inferred increase in bottom-water activity. Geological Society of America Bulletin 84, 2043–2052.

Lawver, L.A., Gahagan, L.M., 1998. Opening of the Drake passage and its impact on Cenozoic ocean circulation. In: Crowley, T.J., Burke, K.C. (Eds.), Tectonic Boundary Conditions for Climate Reconstructions. Oxford Monographs on Geology and Geophysics, vol. 39. Oxford University Press, New York, pp. 121–223.

Lawver, L.A., Royer, J.-Y., Sandwell, D.T., Scotese, C.R., 1991. Evolution of the Antarctic continental margins. In: Thomson, M.R.A., Crame, J.A., Thomson, J.W. (Eds.), Geological Evolution of Antarctica. Proceedings of the Fifth International Symposium on Antarctic Earth Sciences. Cambridge University Press, pp. 533–539.

Lythe, M.B., Vaughan, D.G., the BEDMAP Consortium, 2001. BEDMAP: a new ice thickness and subglacial topographic model of Antarctica. Journal of Geophysical Research 106 (B6), 11335–11351.

Marchant, D.R., Denton, G.H., Swisher III, C.C., Potter Jr., N., 1996. Late Cenozoic Antarctic paleoclimate reconstructed from volcanic ashes in the Dry Valleys region of southern Victoria Land. Geological Society of America Bulletin 108 (2), 181–194.

Martz, L.W., Garbrecht, J., 1998. The treatment of flat areas and depressions in automated drainage analysis of raster digital elevation models. Hydrological Processes 12, 843–855.

McKelvey, B.C., Hambrey, M.J., Harwood, D.M., Mabin, M.C.G., Webb, P.-N., Whitehead, J.M., 2001. The Pagodroma Group—a Cenozoic record of the East Antarctic ice sheet in the northern Prince Charles Mountains. Antarctic Science 13 (4), 455–468.

Mildenhall, D.C., 1989. Terrestrial palynology. In: Barrett, P.J. (Ed.), Antarctic Cenozoic History from the CIROS-1 Drillhole, McMurdo Sound. DSIR Bulletin, 245, 119–127.

Mishra, D.C., Chandra Sekhar, D.V., Venkata Raju, D.Ch., Vijaya Kumar, V., 1999. Crustal structure based on gravity-magnetic modelling constrained from seismic studies under Lambert Rift, Antarctica and Godavari and Mahanadi rifts, India and their interrelationship. Earth and Planetary Science Letters 172, 287–300.

NOAA, 1998. Data Announcement 88-MGG-02, Digital relief of the Surface of the Earth. National Oceanographic and Atmospheric Administration, National Geophysical Data Center, Boulder, Colorado. http://www.ngdc.noaa.gov/mgg/global/seltopo.html. Last Accessed: 11th November 2003.

O'Brien, P.E., Cooper, A.K., Richter, C., et al., 2001. Leg 188 summary: Prydz Bay-Cooperation Sea, Antarctica. Proceedings of the Ocean Drilling Program. Initial Reports 188, 1–65.

Paterson, W.S.B., 2001. The Physics of Glaciers, 3rd edition. Butterworth Heinemann, Oxford.

Raine, Askin, 2001. Terrestrial palynology of Cape Roberts project drillhole CRP-3, Victoria Land Basin, Antarctica. Terra Antartica 8 (3), 389–400.

Ravich, M.G., Fedorov, L.V., 1982. Geologic Structure of MacRobertson Land and Princess Elizabeth Land, East Antarctica. In: Craddock, C. (Ed.), Antarctic Geoscience. Symposium on Antarctic Geology and Geophysics. University of Wisconsin Press, Madison, WI, pp. 499–504.

Robert, C., Kennett, J.P., 1992. Paleocene and Eocene kaolinite distribution in the South Atlantic and Southern Ocean: Antarctic climate and paleoceanographic implications. Marine Geology 103, 99–110.

Ruddiman, W.F., 1977. Late Quaternary deposition of ice-rafted sand in the subpolar North Atlantic (lat 40° to 65°N). Geological Society of America Bulletin 88, 1813–1827.

Rust, D.J., Summerfield, M.A., 1990. Isopach and borehole data as indicators of rifted margin evolution in southwestern Africa. Marine and Petroleum Geology 7, 277–287.

Siegert, M.J., Taylor, J., Payne, A.J., 2005. Spectral roughness of subglacial topography and implications for former ice-sheet dynamics in East Antarctica. Global and Planetary Change 45 (this volume) doi:10.1016/j.gloplacha.2004.09.08.

Stagg, H.M.J., 1985. The structure of Prydz Bay and MacRobertson Shelf, East Antarctica. Tectonophysics 114, 315–340.

Sugden, D.E., Marchant, D.R., Potter Jr., N., Souchez, R.A., Denton, G.H., Swisher III, C.C., Tison, J.-L., 1995. Preservation of Miocene glacier ice in East Antarctica. Nature 376, 412–414.

Summerfield, M.A., Kirkbride, M.P., 1992. Climate and landscape response. Nature 355, 306.

Summerfield, M.A., Hulton, N.J., 1994. Natural controls of fluvial denudation rates in major world drainage basins. Journal of Geophysical Research 99 (B7), 13871–13883.

Tribe, A., 1992. Automated recognition of valley lines and drainage networks from grid digital elevation models: a review and a new method. Journal of Hydrology 139, 263–293.

Zachos, J.C., Breza, J.R., Wise, S.W., 1992. Early Oligocene ice-sheet expansion on Antarctica: stable isotope and sedimentological evidence from Kerguelen Plateau, southern Indian Ocean. Geology 20, 569–573.

Zachos, J.C., Pagani, M., Sloan, L., Thomas, E., Billups, K., 2001. Trends, rhythms, and aberrations in global climate 65 Ma to present. Science 292, 686–693.